Polskie Towarzystwo Materiałów Kompozytowych
Polish Society of Composite Materials

25: 3 (2025) 157–165

COMPOSITES THEORY AND PRACTICE

ISSN (online): 2299-128X

Florian Schmidt *, Marten Walter , Jonas Richter , Sirko Geller , Maik Gude

TUD Dresden University of Technology, Institute of Lightweight Engineering and Polymer Technology, Holbeinstr. 3, 01307 Dresden, Germany
* *Correspondence:* florian.schmidt@tu-dresden.de

Received (Otrzymano) 29.05.2025
Published on-line (Opublikowano) 30.09.2025

OPTIMISATION OF WET WINDING PROCESS PARAMETERS FOR THE PRODUCTION OF TYPE IV HYDROGEN PRESSURE VESSELS WITH HIGH GRAVIMETRIC STORAGE DENSITY

https://doi.org/10.62753/ctp.2025.02.3.3

Wet filament winding is a well-established process to manufacture fibre reinforced polymer (FRP) pressurised vessels. However, due to the large number of process parameters and their interaction, it is difficult to achieve the best component properties from the material system used. For this reason, this article presents an optimisation sequence for setting the individual process parameters, taking into account and prioritising the interactions that occur in each case. The methods employed to optimise the individual process parameters are presented in detail and corresponding production tests were carried out with an exemplary material system. In the course of evaluating the component quality achieved by varying the process parameters using NOL ring tests and analysing micrographs of test specimens, the corresponding optimum process settings for the material system were defined and the achievable component quality was documented.

Keywords: type IV hydrogen pressure vessels, wet filament winding, thermoset processing, process parameter optimisation

INTRODUCTION

In order to decarbonise the aviation industry, green hydrogen will play an important role as a fuel with no CO_2 emissions during its production and use [1-3]. Several possibilities to store hydrogen exist, such as chemically bonding with metal hydrides [4], storage under cryogenic conditions [5] or storage within a pressurised vessel [6].

Of these possibilities, the current state-of-the--art carbon fibre reinforced polymer (CFRP) type IV vessel is a promising approach to store the required amount of hydrogen within an aircraft. Those vessels can be manufactured using the wet filament winding process [7]. Although wet filament winding is a well-established process, there are many, sometimes interdependent, parameters that affect the quality of the produced parts and offer potential for improvement with the goal to produce hydrogen vessels having a higher gravimetric storage density. Researchers like Romagna [8], Błachut et al. [9] or Cohen [10] investigated the influence of several process parameters independently and characterised their individual influence on the component properties. Nevertheless, as the process parameters and their effects on part quality influence each other significantly, it is necessary to develop a selection routine that takes the relevant interactions and dependencies into account.

For this reason, this paper presents a dedicated sequence for selecting suitable production parameters to improve the achievable component properties in the wet winding process, methods for quality evaluation and the results obtained in the course of its implementation.

Wet filament winding process

The state-of-the-art wet filament winding process can be divided into 6 main process steps as shown in Figure 1:

1. Fibre preparation and take-off
2. Fibre impregnation
3. Fibre placement
4. Consolidation
5. Demoulding of the winding core (optional)
6. Reworking and further processing (optional)

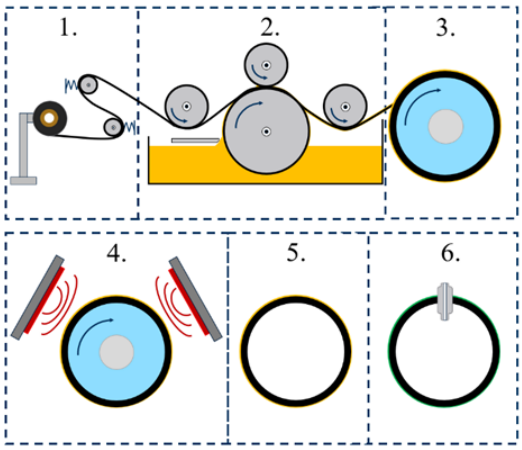

Fig. 1. Steps in conventional state-of-the-art wet filament winding process

In addition to precise fibre placement, fibre impregnation plays a key role in the component quality that can be achieved by means of the manufacturing process. According to Figure 2, two main representatives are currently used for the execution of fibre impregnation in the wet winding process: dip bath impregnation and roller impregnation.

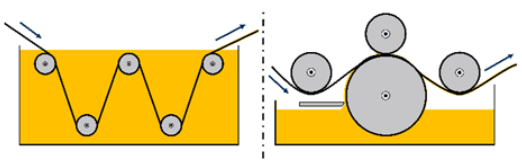

Fig. 2. State-of-the-art impregnation methods: dip bath impregnation (left), roller bath impregnation (right)

While dip impregnation offers advantages in terms of complete filament impregnation due to a longer impregnation time of the filament in combination with an increased number of deflection points within the low-viscosity matrix system, this impregnation concept subjects the filament to greater transverse forces during impregnation owing to smaller deflection radii compared to roller impregnation. This leads to filament damage during the impregnation process, especially in the case of carbon fibres typically used for hydrogen pressure vessels, and thus to a reduction in the achievable mechanical properties of the component. For this reason, the wet winding process employing roller impregnation should be considered for further investigation in the context of hydrogen vessels.

There is a large number of process parameters to be set for this impregnation method. While some of these parameters, such as the roller diameter or the contact angle of the yarn with the roller, are defined by the design as fixed boundary conditions for the existing resin bath, other parameters, such as fibre force F_{fibre} and resin stripper distance h_{rs} within the same resin bath, can be adapted to the particular material system. In addition to this, matrix temperature ϑ_{rb} within the resin bath and fibre take-off speed v_{to} are process parameters to be selected as shown in Figure 3.

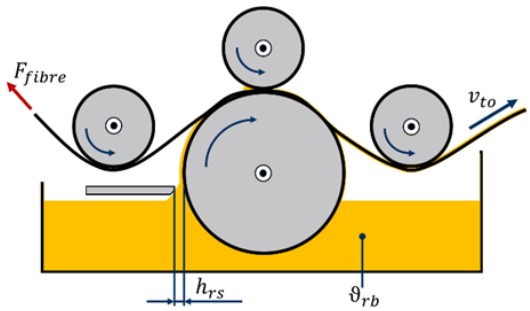

Fig. 3. Process parameters to be optimised in existing resin bath

METHODS AND PROCESS PARAMETER IMPROVISATION SEQUENCE

As already mentioned above, the influence of the process parameters: fibre force F_{fibre}, resin bath temperature ϑ_{rb}, take-off speed v_{to}, and resin stripper distance h_{rs}, are to be evaluated and the corresponding improved settings are to be defined for the material system and process layout used.

For this purpose, the target variables: tensile strength of the composite in fibre direction R_1^+, fibre volume content φ_f and pore content φ_p of the composite produced with the corresponding settings are examined and analysed as evaluation criteria.

As some process parameters have an interactive influence on the achieved component quality, precise test planning must be carried out. For example, increasing the resin bath temperature leads to a reduction in viscosity η of the matrix system, and thus has a direct influence on the impregnation process of the winding thread.

According to Romagna [8], this influences the maximum permissible take-off speed as described in Equation (1):

$$v_{to_{max}} = \frac{S}{\eta} * \frac{\Delta\beta}{h_f} q_s \quad (1)$$

where: $v_{to_{max}}$ = max take-off speed, S = permeability of the thread in thickness direction, $\Delta\beta$ = contact angle of the thread, h_f = thread thickness, q_s = projected tension of the thread

The winding process for the specific part gives a boundary condition in terms of the minimum processing time of the resin system as the resin is not allowed to cure within the resin bath during manufacturing. The temperature dependence of this property suggests determining the minimum pot life at first and then selecting a suitable processing temperature. As a result, the test programme for selecting each process parameter begins with selection of the resin bath temperature and is defined in the following order, as shown in Figure 4, taking into account the occurring interactions.

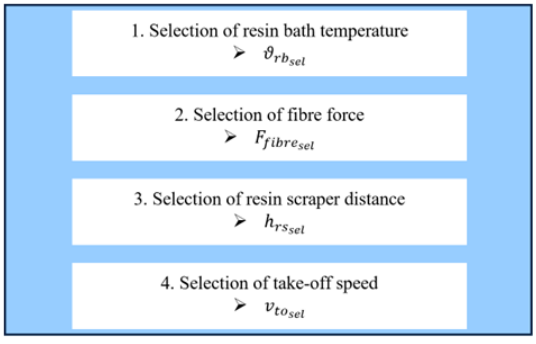

Fig. 4. Sequence of process parameter selection for existing resin bath

Selection of resin bath temperature

To determine a feasible resin bath temperature, it is necessary to define the minimal pot life for processing the resin system. With this requirement defined, rotational rheometer tests shall be carried out to characterise the consolidation behaviour of the resin system. The aim of these tests is to identify the processing temperature at which the viscosity of the matrix system is as low as possible to facilitate thread impregnation, but at which a sufficiently long processing time can be guaranteed.

Selection of fibre force

According to Banerjee et al. [11], the fibre force acting on the wound component during the winding process causes the newly wound layer to compress the underlying layers, and thereby increases the fibre volume content in general. This effect was also observed by Błachut [9]. As the fibres in the component are responsible for transferring the tensile stresses, this should be accompanied by an increase in the tensile strength of the composite in the fibre direction. However, according to Wait et al. [12] a decrease in tensile strength in the direction parallel to the fibres can be observed after a critical fibre stress is exceeded. This is explained by the onset of damage to individual filaments at increased fibre forces, which leads to a decrease in the laminate tensile strength.

In order to qualify this effect and to identify a filament tension that achieves improved component strength for the material system used, tube specimens with a fibre orientation of ≈ 90° are wound with different fibre forces. To reduce the influence of the resin layer that forms unevenly on the outside of the test specimens on the test results, a layer of peel ply is applied as the outermost layer of the test specimens. This layer can be peeled off after the curing process to remove excess matrix material.

The produced tube specimens are then further processed into NOL rings to investigate the influence of the fibre force on part quality. In accordance with ASTM D2290 [13] using a tensile test-

ing machine, the specimens are tested and apparent tensile strength σ_{ats} can be determined. Since a bending load occurs in the free area of the test specimen in addition to the tensile load, apparent tensile strength σ_{ats} determined in this way must be factorized by the occurring overstrength factor o_f according to Equation (2) in order to ascertain the real tensile strength ${R_1}^+$ of the respective test specimen. The overstrength factor depends on the geometry and stiffness of the test specimen and can be determined by means of FEM analysis.

$$ {R_1}^+ = o_f * \sigma_{ats} \tag{2} $$

As part of these tensile tests, the Young's modulus of each specimen is determined by optically measuring the strain in the unbent area utilising an ARAMIS 3D-Camera System. It should be noted that a hysteresis curve is described in the force-displacement diagram due to friction between the specimen and the split disc. Therefore, to acsertain the modulus of elasticity in fibre direction ${E_{II}}^+$, the mean value of the determined modulus of elasticity during loading E_{load} and during unloading E_{unload} must be calculated according to Equation (3).

$$ {E_{II}}^+ = \frac{E_{load}+E_{unload}}{2} \tag{3} $$

Micrographs were taken and analysed in parallel with the tests to ensure good impregnation quality as well as to determine the fibre volume and pore content of the specimens.

The test data was evaluated afterwards. The evaluation criterion used to select fibre force $F_{fibre_{sel}}$ for the following investigations is the achieved tensile strength ${R_1}^+$ in the fibre direction with the aim of maximising this property.

Selection of resin scraper distance

The resin scraper produces a defined resin film thickness to impregnate the winding thread on the impregnating roller. According to Romagna [8], this film thickness should be set slightly supercritical to achieve good impregnation results. Nonetheless, there is no clear evaluation of the pore content as a function of resin film thickness. Furthermore, the influence of the pressure roller was not detailed by Romagna due to a different impregnation setup.

Tubular test specimens with a fibre angle of ≈ 90° and an increased wall thickness are produced with the selected fibre force by varying the resin scraper distance to evaluate the influence on the quality of the component.

For evaluation, micrographs are taken and pore content φ_p of the respective specimens is determined by grey value analysis. Fibre volume content φ_f can be determined by wet chemical analysis. Based on the measured values, a resin scraper distance $h_{rs_{sel}}$ can be defined at which fibre volume content φ_f is high and pore content φ_p is low.

Selection of take-off speed

With the defined optimised resin bath temperature, the fibre tension, resin scraper distance, and the influence of the take-off speed shall be evaluated. For this purpose, according to MIARIS et al. [14], specimens are wound onto a spindle with varying pull-off speeds and analysed using micrographs of samples in the free, non-compressed area. Both single rovings and samples consisting of stacked layers shall be analysed. To ensure that the roving on which the analysed sample section is based has passed through the resin bath at the correct take-off speed, an acceleration section is added to the sample layout. This section is not used for the specimens, but only as a process run-in buffer until the required take-off speed is reached. The specimen layout is shown in Figure 5.

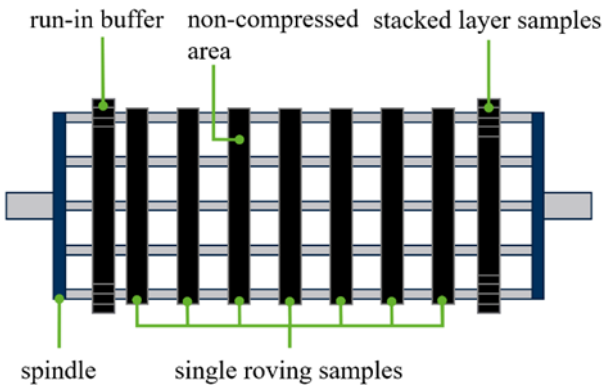

Fig. 5. Principle diagram of sample wound on spindle

The micrographs are examined using grey scale analysis and the resulting pore content φ_p is determined to evaluate the test results. The aim is to achieve a low pore content φ_p while increasing the take-off speed.

EXPERIMENTAL PROCEDURE

The investigations of the influence of the process parameters on part quality during the winding process were performed using Tenax™-E ITS50 F23 24K 1600 tex D supplied by Teijin as a commonly used carbon fibre for hydrogen vessels with good availability. To improve the comparability of the test results, all the production tests were performed using the same coil. In order to establish conservative values for the subsequent design of the pressure vessels, particularly with regard to the optimised fibre-parallel tensile strength of the composite, a coil batch with a comparatively low average fibre tensile strength of 5078.7 MPa was utilised. This must be taken into account when evaluating the measurement results.

The matrix selected for the investigations was the Araldite® LY 3508 Aradur® 917 and the Accelerator DY 070 resin system from Huntsman Advanced Materials.

Selection of resin bath temperature

To investigate the curing behaviour of the selected resin system, rotational rheometer tests were carried out on an Anton Paar Modular Compact Rheometer (MCR) 502. Isothermal tests were performed at the shear rate of $\dot{\gamma} = 100\ s^{-1}$ and temperatures of 40°C, 60°C and 80°C.

Selection of fibre force

In order to analyse the influence of the fibre force on the component quality, pipes with a length of 300 mm were wound with only one thread as described above. With a winding core diameter of 100 mm and a thread deposit width of 6 mm, this results in a fibre angle of 88.91° for the circumferential layers. In order to not negatively influence the impregnation quality of the test specimens, the tubes were produced at a low take-off speed of 5 m/min (compared to section 3.4) and with a resin scraper distance of 0.3 mm. The influence of the thread force was investigated in a total of five test series with fibre forces of 3 N, 11 N, 20 N, 30 N and 40 N. They were set and continuously regulated by the used bobbin stand that also specified fibre forces of 3 N and 11 N by the possible adjustment steps of the machine equipment.

The tubes produced in this way were cut into NOL rings with a test specimen width of 9 mm employing a high-precision water-cooled AXITOM cutting machine. For each fibre force, 12 test specimens were tested on an UPM Zwick 1465 equipped with a 50 kN load cell at the test speed of 1 mm/min.

Selection of resin scraper distance

With set $\vartheta_{rb_{sel}}$ and $F_{fibre_{sel}}$, the influence of resin scraper distance h_{rs} was investigated. To identify a suitable setting, resin scraper distances 0.125 mm, 0.175 mm, 0.225 mm, 0.325 mm and 0.425 mm were analysed. With these settings, pipe test specimens were produced in accordance to the production parameters of NOL ring specimens but with 12 individual layers, a resulting thickness of approx. 3 mm, and without a peel ply. Two rings were cut for each setting. Microscopic specimens of 2 mm x 1 mm were taken from each of these rings at four locations and were examined using grey scale analysis, giving eight specimens per sample configuration.

Selection of take-off speed

In the course of the tests in order to optimise the take-off speed, test specimens were produced according to the procedure described in section 2.4 with the already selected process parameters and take-off speeds of 5 m/min; 10 m/min; 15 m/min; 20 m/min and 30 m/min.

RESULTS

Selection of resin bath temperature

Although the resin system is used up repeatedly during the winding process and must be refilled accordingly, it cannot be ruled out that components of the resin system, particularly in the

flow-calmed zones of the resin tank, may remain for a longer period of time and cure completely. Since this would lead to an unwanted process interruption and as the winding process of a pressurised hydrogen tank, which is relevant for the investigations, takes more than one working day, the minimum pot life of the resin system to be observed was set to 8 hours. This corresponds to the daily working time of one operator and thus to the maximum expected continuous winding time before resin bath cleaning. As shown in Figure 6, this pot life can only be safely guaranteed at a resin bath temperature of 40°C. For this reason, 40°C is defined as resin bath temperature $\vartheta_{rb_{sel}}$ for further investigations.

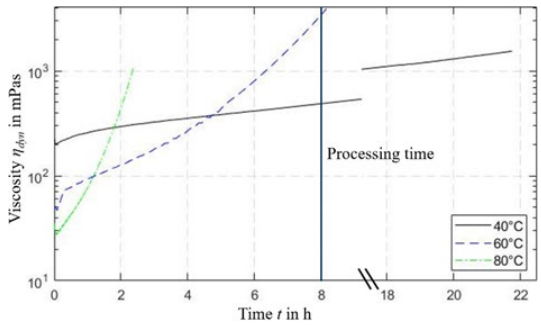

Fig. 6. Rotational rheometer measurement data for used resin system

Selection of fibre force

The determined mechanical properties of the test specimens produced according to the described procedure in 3.2. are shown in Figure 7.

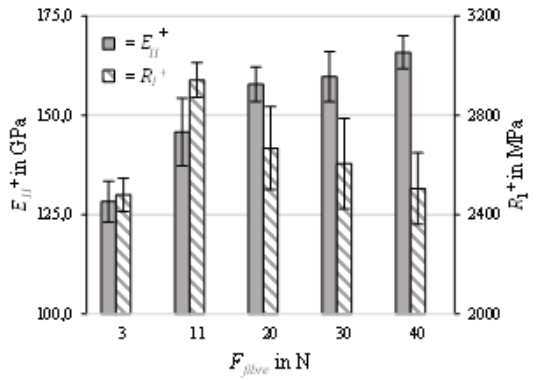

Fig. 7. Tensile strength R1+and modulus of elasticity EII+ of test specimens produced under variation of fibre force Ffibre determined by split-disc testing

The maximum of the average tensile strength of the composite of 2942.11 MPa occurs at the thread force of 11 N. At higher thread force settings, however, decreasing strength is observed despite a degressively increasing modulus of elasticity of the test specimens. It is assumed that this tendency is caused by the increase of fibre damage at higher fibre forces. The observed higher amounts of broken individual filaments accumulating at the deflection points of the thread eye during the production of the test specimens with 40 N fibre force underline this assumption. This reasoning suggests that filament damage occurs with lower intensity, and therefore less visible even at lower fibre force settings.

On the other hand an increment in filament force results in higher fibre volume contents, as can be seen in figure 8. Nonetheless, this positive effect is offset by the increase in the number of broken individual filaments at higher thread forces. Those broken filaments contribute less to the tensile strength of the specimen, and therefore reduce component strength in the fibre direction. Eventually, at a specific fibre force between 3 N and 20 N the positive effect on the tensile strength in the fibre direction of increasing fibre volume content is overtaken by the negative influence of filament damage, and results in a lower tensile strength.

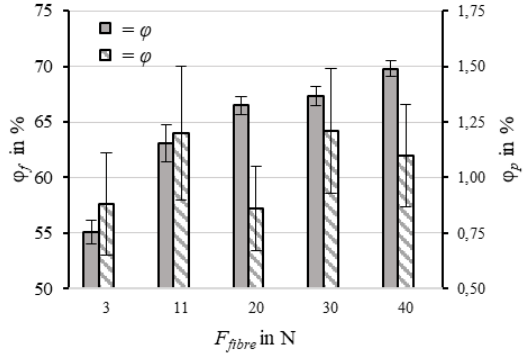

Fig. 8. Fibre volume content φf and pore content φp of test specimens produced under variation of fibre force Ffibre

Since the maximum tensile strength of the composite in the fibre direction was defined as the main objective of the tests, the selected fibre force $F_{fibre_{sel}}$ within the test series is 11 N.

While the fibre volume content also shows a degressive increase as a function of the fibre force, no direct correlation between the fibre force and pore content can be determined within the series of measurements as displayed in Figure 8.

Selection of resin scraper distance

According to the results shown in Figure 9, the lowest minimum mean pore content of 1.4% ± 0.24% occurs at the resin scraper spacing of 0.175 mm.

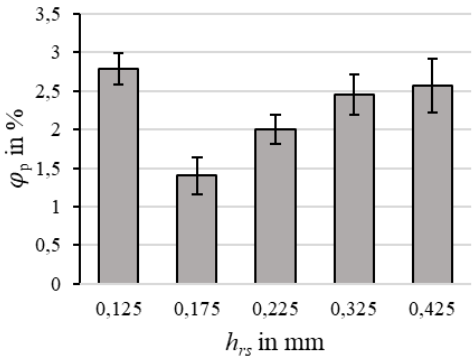

Fig. 9. Influence of resin scraper distance hrs on pore content φp

It is assumed that the higher proportion of pores at a higher resin scraper distance is caused by the resin bead on the pressure roller, which grows at increasing resin scraper distances. As visualised in Figure 10, the resin bead progressively accumulates more air bubbles on closer inspection, which are probably introduced into the winding thread during the impregnation process. These entrapped bubbles remain to some extent in the wound part and therefore cause a higher proportion of pores in the test specimen if the resin scraper distance is set too high.

On the other hand, if the resin scraper distance is set too low, the impregnation unit is not able to deliver enough resin for complete thread impregnation. Spots within the thread remain dry during fibre placement and consolidation, and result in higher pore contents as well.

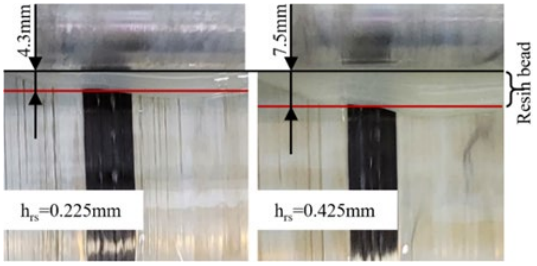

Fig. 10. Comparison of resulting resin bead with different resin scraper distances

In the course of the wet-chemical investigation to determine the fibre volume content, no clear correlation could be identified between the fibre volume fraction or resin content and the set resin scraper distance.

In summary, owing to the lowest pore content and the non-apparent influence on the fibre volume and resin content, $h_{rs_{sel}} = 0.175\ mm$ was set as the chosen resin scraper distance under the defined boundary conditions.

Selection of take-off speed

Although the test series was planned to investigate take-off speeds from 5 to 30 m/min, the studies for the take-off speed of 30 m/min had to be cut short: the impregnation roller was spinning too fast, resulting in the resin system being sprayed off of the same.

Between the 10 samples produced at each take-off speed and those with single impregnated rovings, no significant differences in the resulting pore content were observed. Instead, the single layer samples exhibited almost perfect impregnation properties with no pores within the sample. Nevertheless, this result was not observed for the stacked layer specimens with n = 12 layers. As an example, Figure 11 compares single layer specimens produced at the take-off speeds of 5 m/min and 20 m/min with a stacked layer specimen produced at the take-off speed of 20 m/min. Both samples with single impregnated roving have a very good impregnation quality, while the layered specimen has visible pores.

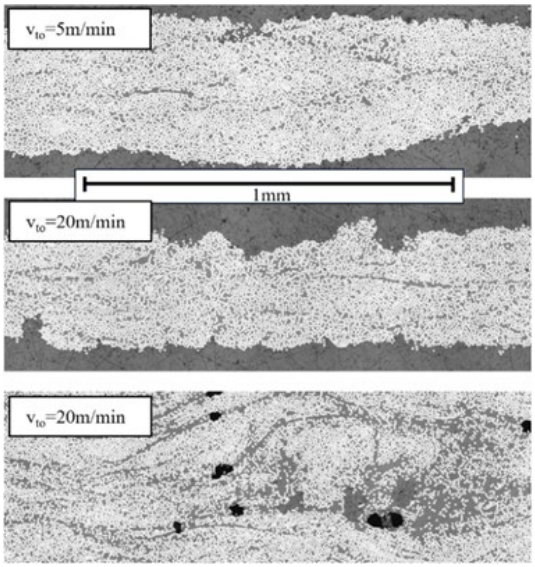

Fig. 11. Comparison of impregnation quality of single layer specimens wound at 5 and 20 m/min take-off speed and stacked test specimen wound at 20 m/min (top to bottom)

Within the stacked test specimens, a clear increase in pore content can be seen with increasing take-off speed: while a pore content of 1.47% ± 0.29% was achieved at the take-off speed of 5 m/min, the average pore content at the take-off speed of 20 m/min was 2.38% ± 0.29% as shown in Figure 12 for n=18 test samples.

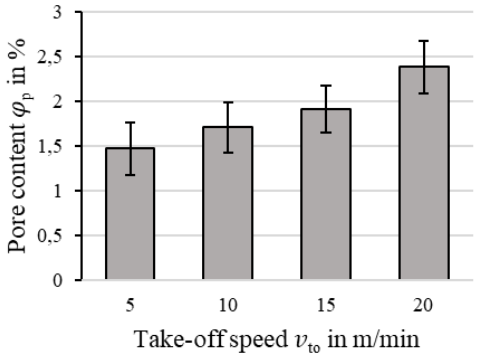

Fig. 12. Influence of take-off speed vto on pore content φp

Based on this result, it is assumed that the low pore content within the individual roving tests provides irrelevant results as a consequence of an outgassing effect that occurs during the consolidation phase. The pores introduced during impregnation of the roving are squeezed out of the roving in the course of consolidation at elevated temperatures, which falsifies the actual pore content. This theory is supported by the fact that the stacked test specimens edge areas have little to no pores, while centrally located test specimen sections do have pores, especially in resin-rich areas. This effect has also been described by Lasn et al. [15], and can therefore be assumed to occur for the single layer specimens.

In summary, for the selection of a take-off speed, 20 m/min can be defined as the upper limit that should not be exceeded during the winding process with the impregnation setup used, in order to reduce the risk of resin spraying. The take-off speed can therefore be set to up to 20 m/min, but this directly affects part quality. While the lowest pore content and highest part quality were achieved at the take-off speed of 5 m/min in the test series, higher productivity can be achieved at the expense of higher pore content at elevated take-off speeds.

CONCLUSIONS AND OUTLOOK

Significant improvements in terms of component quality were achieved with the help of the presented sequence of process parameter selection. While the investigated resin stripper distance $\boldsymbol{h_{rs}}$ and take-off speed $\boldsymbol{v_{to}}$ have a particular influence on the pore content of the manufactured test specimens, filament force $\boldsymbol{F_{fibre}}$ was identified as the most important influencing factor for the achievable fibre volume content φf, tensile strength $\boldsymbol{R_1}^+$ as well as Young's modulus $\boldsymbol{E_{II}}^+$ in the fibre direction of the test specimens. With the selected thread force $\boldsymbol{F_{fibre_{sel}}}$ of 11 N, a significant rise in the maximum tensile strength in the fibre direction of 19% (3 N) and 9% (20 N) was achieved compared to the next level of thread force investigated. This significant growth in the tensile strength in the fibre direction contributes to an increase in the gravimetric storage density of isotensoid hydrogen pressure tanks in particular.

However, as the fibre force with the machine used for the winding process can only be set at the bobbin stand and yet cannot be measured directly

at the deposit point, these results can only be transferred to other winding systems to a limited extent. For this reason, concepts for fibre force measurement close to the deposit point are to be evaluated and applied for further investigations. In addition, the effects that occur during fibre impregnation need to be further investigated and improved with the goal to increase productivity and repeatability while achieving the same level of component quality.

Funding

Funding was provided by the German Federal Ministry for Economics and Climate Action (BMWK) on the basis of decisions by the German Bundestag within the joint research project "SWaT" (grant number 20M2112F).

REFERENCES

[1] Yusaf T., Fernandes L., Abu Talib A.R., Altarazi Y.S.M., Alrefae W., Kadirgama K., Ramasamy D., Jayasuriya A., Brown G., Mamat R., et al., Sustainable Aviation – Hydrogen Is the Future. Sustainability 14, no. 1: 548. 2022.

[2] Afonso F., Sohst M., Diogo C., Rodrigues S., Ferreira A., Ribeiro I., Marques R., Rego F., Sohouli A., Portugal-Pereira J., Policarpo H., Soares B., Ferreira B., Fernandes E., Lau F., Suleman A., Strategies towards a more sustainable aviation: A systematic review, Progress in Aerospace Sciences, Volume 137, 2023.

[3] Maciorowski D., Ludwiczak A, Kozakiewicz A. Hydrogen, the future of aviation. Combustion Engines. 2024;197(2):126-131.

[4] Franke F., Kazula S., Enghardt L. Elaboration and outlook for metal hydride applications in future hydrogen-powered aviation. The Aeronautical Journal. 2024.

[5] Aceves S., Espinosa-Loza F., Ledesma-Orozco E., Ross T., Weisberg A., Brunner T., Kircher O., High-density automotive hydrogen storage with cryogenic capable pressure vessels, International Journal of Hydrogen Energy, Volume 35, Issue 3, 2010.

[6] Schlegel D., Schmidt F., Birke M., Spitzer S., Gude M., Aerodynamic high-pressure hydrogen CFRP vessels with increased storage energy density: method for the optimization of a manufacturable laminate, Proceedings of the 2023 International Conference on Composite Materials (ICCM23), 2023.

[7] Ramirez J., Halm D., Grandidier J.-C., Villalonga S., Nony F., 700 bar type IV high pressure hydrogen storage vessel burst – Simulation and experimental validation, International Journal of Hydrogen Energy, Volume 40, Issue 38, 2015.

[8] Romagna J., Neue Strategien in der Faserwickeltechnik, Dissertation, Eidgenössische Technische Hochschule Zürich, 1997.

[9] Błachut A., Wollmann T., Panek M., Vater M., Kaleta J., Detyna J., Hoschützky S., Gude M., Influence of fiber tension during filament winding on the mechanical properties of composite pressure vessels, Composite Structures, Volume 304, Part 1, 2023.

[10] Cohen D., Influence of filament winding parameters on composite vessel quality and strength, Composites Part A: Applied Science and Manufacturing, Volume 28, Issue 12, 1997.

[11] Banerjee A., Sun L., Mantell S.C., Cohen D., Model and experimental study of fiber motion in wet filament winding, Composites Part A: Applied Science and Manufacturing 29A, 1998.

[12] Wait C.F., Clean filament winding: industrial site trials and product evaluation, Dissertation, University of Birmingham, 2015.

[13] ASTM D2290: Standard Test Method for Apparent Hoop Tensile Strength of Plastic or Reinforced Plastic Pipe by Split Disk Method, ASTM International, 2000.

[14] Miaris A., Paessler M., Lichtner J., Schledjewski R., Siphon impregnation: The development of a new method for impregnation during filament winding, International Conferences on Composite Materials, 2009.

[15] Lasn K., Mulelid M., The effect of processing on the microstructure of hoopwound composite cylinders, Journal of Composite Materials 54.26, 2020.

